JOURNAL OF OCULAR PHARMACOLOGY AND THERAPEUTICS
Volume 27, Number 2, 2011

DOI: 10.1089/jop.2010.0188

Ocular Sustained Release Nanoparticles Containing Stereoisomeric Dipeptide Prodrugs of Acyclovir

Jwala Jwala,[1] Sai H.S. Boddu,[2] Sujay Shah,[1] Suman Sirimulla,[3] Dhananjay Pal,[1] and Ashim K. Mitra[1]

Abstract

Purpose: The objective of this study was to develop and characterize polymeric nanoparticles of appropriate stereoisomeric dipeptide prodrugs of acyclovir (L-valine-L-valine-ACV, L-valine-D-valine-ACV, D-valine-L-valine-ACV, and D-valine-D-valine-ACV) for the treatment of ocular herpes keratitis.
Methods: Stereoisomeric dipeptide prodrugs of acyclovir (ACV) were screened for bioreversion in various ocular tissues, cell proliferation, and uptake across the rabbit primary corneal epithelial cell line. Docking studies were carried out to examine the affinity of prodrugs to the peptide transporter protein. Prodrugs with optimum characteristics were selected for the preparation of nanoparticles using various grades of poly (lactic-co-glycolic acid) (PLGA). Nanoparticles were characterized for the entrapment efficiency, surface morphology, size distribution, and *in vitro* release. Further, the effect of thermosensitive gels on the release of prodrugs from nanoparticles was also studied.
Results: L-valine-L-valine-ACV and L-valine-D-valine-ACV were considered to be optimum in terms of enzymatic stability, uptake, and cytotoxicity. Docking results indicated that L-valine in the terminal position increases the affinity of the prodrugs to the peptide transporter protein. Entrapment efficiency values of L-valine-L-valine-ACV and L-valine-D-valine-ACV were found to be optimal with PLGA 75:25 and PLGA 65:35 polymers, respectively. *In vitro* release of prodrugs from nanoparticles exhibited a biphasic release behavior with initial burst phase followed by sustained release. Dispersion of nanoparticles in thermosensitive gels completely eliminated the burst release phase.
Conclusion: Novel nanoparticulate systems of dipeptide prodrugs of ACV suspended in thermosensitive gels may provide sustained delivery after topical administration.

Introduction

Ocular herpes is a persistent viral infection caused by the herpes simplex virus-1 (HSV-1). It is one of the most common infectious diseases causing corneal blindness in the United States. HSV-1 infections can be mainly classified into HSV neonatal, HSV encephalitis, and HSV keratitis. Subsequent to the primary ocular infection, HSV-1 can establish latency in the trigeminal ganglia throughout the lifetime of the host. Intermittent corneal infections can lead to corneal thinning, scarring, stromal opacity, and ultimately, blindness.[1,2] Previous studies demonstrate that patients infected with HSV-1 have a 50% chance of recurrence.[3]

Herpes simplex keratitis is characterized by rapid spread of virus deep into the cornea and develops into a more severe infection called stromal keratitis, which renders the body's immune system attack and destroy stromal cells. Recurrent episodes of stromal keratitis often results in corneal scarring, thereby leading to vision loss.[4,5] Statistics reveal that every year 50,000 cases are reported in the United States. Acyclovir (ACV) is an antiviral drug with high specificity against herpes viruses, and it is the drug of choice for treatment of ocular herpes infections.[6] Topical treatment of ACV in the form of ointment has been proved to be effective in the treatment of superficial HSV keratitis.[7] However, its use in the United States has not been approved by the Food and Drug Administration (FDA) due to side effects associated with this formulation; and the treatment fails especially when deeper ocular tissues are involved such as stromal keratitis. A compound should possess optimum hydrophilicity and lipophilicity for 2 reasons: (1) to allow sufficient permeability across the corneal layers; (2) sufficient solubility suitable for eye drops. ACV is a hydrophilic drug with poor aqueous solubility (0.2 mg/mL) and low corneal permeability.[5,8]

[1]Division of Pharmaceutical Sciences, School of Pharmacy, University of Missouri-Kansas City, Kansas City, Missouri.
[2]Department of Pharmacy Practice, The University of Toledo, Toledo, Ohio.
[3]Department of Chemistry, University of Texas at El Paso, El Paso, Texas.

Many attempts have been made to increase the corneal penetration of ACV. One of the most widely used approaches is prodrug derivatization. Corneal permeability of ACV has been significantly improved with acyl ester prodrugs.[8] However, enhanced lipophilicity and resulting poor solubility prohibited the formulation of 1%–3% eye drops. Later, dipeptide prodrugs of ACV such as glycine-valine-ACV (GVACV), valine-valine-ACV (VVACV), and valine-tyrosine-ACV (VYACV) were designed to target the oligopeptide transporter (PEPT), which is widely expressed on the cornea.[9] These dipeptide prodrugs (GVACV and VVACV) were found to be more permeable due to specific targeting toward PEPT and are considered as the potential candidates for the treatment of ocular HSV infections.[10] Talluri et al. synthesized stereoisomeric dipeptide prodrugs of ACV such as L-valine-L-valine-ACV (LV-LV-ACV), L-valine-D-valine-ACV (LV-DV-ACV), D-valine-L-valine-ACV (DV-LV-ACV), and D-valine-D-valine-ACV (DV-DV-ACV) and evaluated permeability across Caco-2 cell monolayer.[9] However, the effect of stereoisomerism in the ocular delivery of ACV has not yet been explored.

Successful design of an ocular drug delivery system requires (1) optimal physicochemical properties of drugs; and (2) drug residence in the precorneal area for an extended period of time. Conventional dosage forms such as solutions and suspensions can produce subtherapeutic drug levels due to rapid loss through tear turnover and blink reflux in precorneal area.[11] Moreover, conventional dosage forms such as eye drops should be administered frequently to achieve the required ocular bioavailability. Alternative drug delivery systems such as ophthalmic inserts are currently indicated to overcome the disadvantages associated with conventional dosage forms. Blurred vision and discomfort can result in some degree of noncompliance with ophthalmic inserts.

An ideal ocular drug delivery system should possess good loading capacity, ability to reside in the precorneal area for a substantial period, and capacity to release the drugs in a controlled manner.[12] Colloidal nanocarriers made up of biodegradable polymeric materials have been successfully employed to enhance intraocular drug penetration and controlled release. However, the major limitation with polymeric nanocarriers is short residence in the precorneal area.[13]

In this article, we report alternative strategies for increasing the overall therapeutic efficacy of the ACV-prodrugs after topical administration. The stereoisomeric peptide prodrugs of ACV (LV-LV-ACV, LV-DV-ACV, DV-LV-ACV, and DV-DV-ACV) were evaluated for bioreversion in corneal cell and tissue homogenates. Uptake was conducted in the rabbit primary corneal epithelial cell (rPCEC) line. Docking studies were carried out to examine the affinity of prodrugs to the peptide transporter protein. Prodrugs with optimum stability and affinity toward PEPT on the cornea were loaded into PLGA nanoparticles. Effect of lactide/glycolide ratio on the prodrug entrapment efficiency was evaluated. Nanoparticles with optimum entrapment efficiency were characterized for size, surface morphology, zeta potential, and *in vitro* release properties. We have also investigated the effects of PLGA-PEG-PLGA thermosensitive gel on the release of prodrugs from PLGA nanoparticles.

Materials

ACV, [9-(2-hydroxyethoxymethyl) guanine] was obtained as a gift from Burroughs Wellcome Co.; and Val-ACV was a gift from GlaxoSmithKline. All the stereoisomeric dipeptide prodrugs of ACV were synthesized and purified in our laboratory. [3H]-Glycylsarcosine (Gly-Sar-4 Ci/mmol) was procured from Moravek Biochemicals. rPCECs were cultured in our laboratory. The growth medium, that is, minimal essential medium was procured from Invitrogen. Penicillin, streptomycin, lactalbumin enzymatic dehydrolysate, sodium bicarbonate, and HEPES were purchased from Sigma-Aldrich. Calf-serum was obtained from Atlanta biologicals. Culture flasks (75-cm^2 growth area) and 12-well Costar® plates, all buffer components, and solvents were purchased from Fisher Scientific Co. PLGA polymers, that is, PLGA 50:50 (D,L-lactide:glycolide) with molecular weight (M_w) 45,000–75,000 Da; PLGA 65:35 (D,L-lactide:glycolide), with a M_w of 45,000–75,000 Da; PLGA 75:25 (D,L-lactide:glycolide) with a M_w of 66,000–107,000 Da; PLA (L-lactide) with a M_w of 85,000–160,000; and polyvinyl alcohol (PVA) were purchased from Sigma Chemicals. Thermosensitive gel PLGA-PEG-PLGA [weight average molecular weight (M_{wb}) 4,759 Da] was synthesized and purified in our lab. Cell Titer 96® Aqueous NonRadioactive Cell Proliferation Assay kit was procured from Promega. Distilled deionized water was used in the preparation of all buffers and mobile phase. Sodium pentobarbital was obtained from the stock maintained by the UMKC school of Pharmacy and used under supervision. All other required chemicals were obtained from Sigma-Aldrich Company.

Methods

Synthesis

Stereoisomeric dipeptide prodrugs of ACV (LV-LV-ACV, LV-DV-ACV, DV-LV-ACV, and DV-DV-ACV) were synthesized according to a previously published procedure with minor modifications.[14] The products obtained were purified by silica gel column chromatography and were deprotected using trifluoroaceticacid. These compounds were recrystallized using cold diethyl ether. The progress of the reaction was monitored with thin layer chromatography (TLC) and liquid chromatography tandem mass spectrometry (LC-MS/MS). The structures of the intermediate and final compounds were confirmed by ^{1}H NMR and mass spectrometry.^{1}H NMR was carried out using a Varian-400 MHz NMR spectrometer. Chemical shifts were expressed in parts per million (ppm) relative to the solvent signal (CD_3OD, 3.31ppm for proton) using tetramethylsilane as an internal standard. Mass spectroscopy was carried out by a hybrid triple quadrupole linear ion trap mass spectrometer (Q trap LC-MS/MS spectrometer, Applied Biosystems-2000). An enhanced mass spectrum (EMS) mode was used for the conformation of intermediates and final compounds.[15]

Animals

Rabbits (New Zealand albino adult male) weighing between 2.0 and 2.5 kg were procured from Myrtle's Rabbitry. All animal studies were conducted according to the ARVO guidelines for the use of animals in vision research.

Cell culture

rPCEC line with a passage number of 10 was utilized. The culture medium contained minimum essential medium supplemented with 10% calf serum (non heat inactivated),

100 U/L of penicillin, 100 U/L of streptomycin, 1.76 g/L lactalbumin enzymatic dehydrolysate, and 1.3 g/L HEPES. Cells were grown and maintained in a humidified incubator at 37°C with 5% carbon dioxide in air atmosphere. At 100% confluence, cells were harvested by treating with Tripple Express (Invitrogen); and then, 250,000 cells per each well were added to 12-well tissue culture plastic plates. These cells were grown for 10–11 days and utilized for uptake studies. The culture medium was replaced every alternate day during the growth period.[16]

Prodrugs stability in rPCEC and rabbit ocular tissue homogenates

Hydrolysis of prodrugs was performed in cell and ocular tissue homogenates. The method is described in the following sections.

Preparation of cell and ocular tissue homogenates

Rabbits were euthanized by administering sodium pentobarbital (50 mg/kg) through the marginal ear vein. Each eye was instantly enucleated, and ocular surface was rinsed with ice-cold, isotonic phosphate-buffered saline (IPBS of pH 7.4) to remove any traces of blood. Aqueous humor was removed with a 27G needle attached to a 1 mL tuberculin syringe; and then cornea, lens, and iris ciliary body were removed sequentially by cutting along the scleral-limbus junction. Aqueous humor and other ocular tissue samples were stored at −80°C before any experiment. Tissues were homogenized in 5 mL chilled (4°C) IPBS for about 4 min with a tissue homogenizer (Tissue Tearor, Model 985-370; Dremel Multipro) in an ice bath. Similarly, rPCECs were also homogenized in 5 mL chilled (4°C) IPBS for about 4 min. Later, the homogenates and aqueous humor were centrifuged separately at 12,500 rpm for 25 min at 4°C to remove cellular debris; and the supernatant was used for hydrolysis studies. Protein content of each supernatant was estimated with a BioRad assay with bovine serum albumin as the standard.[17]

Bioreversion studies

The supernatant containing 0.5 mg/mL protein content (1.2 mL) was equilibrated at 34°C for about 30 min before an experiment. Hydrolysis was initiated by the addition of 300 μL of 1 mM prodrug solution to the supernatant, which is placed in a shaking water bath set at 34°C and 60 rpm. Samples (100 μL) were withdrawn at appropriate time intervals into microcentrifuge tubes prefilled with 100 μL of ice-cold organic mixture containing acetonitrile and methanol (4:5) to precipitate the cellular and tissue proteins as well as to stop the reaction. The samples were stored at −80°C until further analysis was carried out. Analysis was performed by high-performance liquid chromatography (HPLC). The samples were thawed and centrifuged to remove any precipitated protein. The supernatant was injected into HPLC. The apparent first-order degradation rate constants were calculated from the slope of log (prodrug concentration) versus time plots. It is corrected for any chemical hydrolysis observed with the control.[10,18]

Modeling of rabbit PEPT1 protein

The entire rabbit PEPT1 protein sequence (P36836) was retrieved from the UNIPPROT database.[19] The sequence was submitted to I-Tasser homology model-building server for model calculation.[20–22] Stereo chemical quality check was performed on the returned model. A few problematic side chain conformations and missing amino acids were identified and rectified using prime.[22] The resulting structure was prepared using protein preparation wizard and energy minimized using OPLS 2005 force field.[23]

Docking of ACV peptide prodrugs

The structure of ACV peptides was sketched using maestro[24] and prepared using Ligprep.[25] Glide[26] (molecular docking program from Schrodinger, Inc.) was engaged to perform the docking studies with standard default settings. Receptor grid generation file was generated by defining the binding site to include all atoms within 20 Å of TRP 294, as TRP 294 is known to be involved in initial binding of peptides.[27] An extra precession docking was performed with the 4 ACV peptide prodrugs using the grid file prepared by the above-explained process. GlideScore (GScore)[28–30] is based on ChemScore, but includes a steric-clash term, adds buried polar terms devised by Schrödinger to penalize electrostatic mismatches, and has modifications to other terms:

GScore = 0.065*VDW + 0.130*Coul + Lipo + HBond + Metal + BuryP + RotB + Site

Binding affinity varies inversely with GScore meaning; the lower the GScore, the stronger is the binding affinity. The components of the GlideScore are described as

Van der Waals energy (VDW): This term is calculated with reduced net ionic charges on groups with formal charges, such as metals, carboxylates, and guanidiniums.

Coulomb energy (Coul): This term is calculated with reduced net ionic charges on groups with formal charges, such as metals, carboxylates, and guanidiniums.

Lipophilic (Lipo): term derived from hydrophobic grid potential. Rewards favorable hydrophobic interactions.

Hydrogen-bonding term (HBond): This term is separated into differently weighted components that depend on whether the donor and acceptor are neutral; one is neutral and the other is charged, or both are charged.

Metal-binding term (Metal): Only the interactions with anionic acceptor atoms are included. If the net metal charge in the apo protein is positive, the preference for anionic ligands is included; if the net charge is zero, the preference is suppressed.

BuryP: Penalty for buried polar groups

RotB: Penalty for freezing rotatable bonds

Site: Polar interactions in the active site. Polar but non-hydrogen-bonding atoms in a hydrophobic region are rewarded.

Cytotoxicity studies

Cytotoxicity of all stereo isomeric dipeptide prodrugs was determined with an aqueous nonradioactive cytotoxicity kit based on the MTT assay. The assay examines cell viability based on the principle of mitochondrial conversion of a water-soluble tetrazolium salt [3-(4, 5-dimethylthiazol-2-yl)-2,5-diphenyltetrazolum bromide; MTT] to the water-insoluble blue formazan product. The cytotoxicity kit is supplied as a salt solution of MTT that is composed of MTS [3-(4,5-dimethylthiazol-2-yl)-5-(3-carboxymethoxyphenyl)-2-(4-sulfophenyl)-2H-tetrazolium] and phenazine methosulfate (PMS). PMS has enhanced chemical stability, which allows it to be combined with MTS to form a stable solution eliminating the need to solubilize formazan crystals by an external means. rPCECs were grown in

96-well tissue culture plates at 10,000 cells per well density over a period of 24 h before drug treatment. Culture medium was then removed and replaced with 100 μL medium containing serial dilutions of the prodrugs (1–5 mM). Cells were then incubated for 24 h at 37°C under 5% CO_2. At the end of the treatment period, medium was aspirated, rinsed with PBS, and 20 μL of MTS containing PMS stock solution was added to each well. After the addition of the MTS dye, cells were incubated for 4 h at 37°C. Cell viability was then measured by absorbance at 485 nm on an automated plate reader (BioRad). The quantity of formazan product was measured at 485 nm, and the absorbance is directly proportional to the number of living cells in the culture.[16,17]

Uptake studies

Uptake studies were conducted with confluent rPCECs. Cells were washed thrice with DPBS after aspirating the medium from each well. All the drug and prodrug solutions were added before the experiment. ACV and peptide prodrugs (1, 2.5 and 5 mM of LV-LV-ACV, LV-DV-ACV, DV-LV-ACV, and DV-DV-ACV) were dissolved in DPBS. Control solutions contained only DPBS. The study was initiated by adding 1 mL of drug or prodrug solution containing 0.5 μCi/mL of [^{3}H] Gly-Sar (GS) to the wells. Incubation was carried out over a period of 30 min at 37°C. Cells were washed thrice with ice-cold stop solution and then lysed overnight with 1 mL 0.1% (w/v) Triton X-100 in 0.3N sodium hydroxide at room temperature. Aliquots (200 μL) were withdrawn from each well and transferred to vials containing 3 mL scintillation cocktail. All samples were analyzed with a Beckman scintillation counter (Model LS-6500; Beckman Instruments, Inc.). Uptake was normalized to the protein content of that specific well. Amount of protein in the cell lysate was estimated by a Bio-Rad protein estimation kit (Bio-Rad).[31]

Analytical procedure

Drug and prodrug samples were assayed by reversed phase HPLC as per the previously published procedure.[15] The HPLC system comprised of a Rainin Dynamax Pump SD-200, HP 1100 series fluorescence detector set at an excitation wavelength of 285 nm and an emission wavelength 360 nm. Alcott auto sampler Model 718 AL and a C18 Luna column 4.6×250 mm (Phenomenex) were utilized. The mobile phase consisted of 25 mM ammonium phosphate buffer (pH adjusted to 2.5): acetonitrile: (95:5), at a flow rate of 1 mL/min. This method gave rapid and reproducible results. Limits of quantification were found to be ACV: 50 ng/mL; LV-ACV and DV-ACV: 300 ng/mL; and LV-LV-ACV, LV-DV-ACV, DV-LV-ACV, and DV-DV-ACV: 500 ng/mL. Variation among intra- and inter-day precision (measured by coefficient of variation) was less than 3% and 4%, respectively.

Preparation of nanoparticles by water in oil in water method

Nanoparticles were prepared by water in oil in water (W/O/W) emulsion solvent evaporation method. Prodrugs (LV-LV-ACV and LV-DV-ACV) were dissolved in an aqueous solution that forms an internal aqueous phase. This solution was then emulsified in an organic solution containing PLGA polymer to form a primary emulsion. The primary emulsion was sonication (Fisher 100 Sonic Dismembrator; Fisher Scientific) at a constant power output of 55W for 2 min. Organic phase was slowly mixed with an aqueous solution containing 2.5%w/v PVA under continuous stirring.[32] A W/O/W type emulsion was formed on sonication at a constant power output of 55W for 5 min. The sample was kept in an ice bath during sonication to prevent any overheating of the emulsion. The mixture was stirred gently at room temperature for 3 h. Subsequently, nanoparticle suspension was subjected to vacuum for 1 h to ensure complete removal of organic solvents. Un-entrapped prodrug and PVA residue were removed by washing nanoparticles thrice with distilled deionized water. The resultant suspension was centrifuged at 22,000 g for 60 min. Nanoparticles formed were freeze-dried over 48 h.[12]

Entrapment and loading efficiencies

For measuring prodrug entrapment in nanoparticles, 1 mg of freeze-dried sample was dissolved in 2 mL of dichloromethane and mixed thoroughly for 24 h. Subsequently, these samples were dried under inert atmosphere and subsequently dissolved in 200 μL acetonitrile: water (70:30) and centrifuged at 12,000 *g* for 10 min. The supernatant was analyzed for prodrug content by HPLC. Entrapment efficiency and prodrug loading were calculated by Eqs. 1 and 2.

$$\text{Entrapment efficiency (\%)} = \frac{\text{Amount of prodrug remained in nanoparticles}}{\text{Initial prodrug amount}} \times 100 \quad \text{Eq.1}$$

$$\text{Drug loading (\%)} = \frac{\text{Weight of prodrug in nanoparticles}}{\text{Weight of nanoparticles}} \times 100 \quad \text{Eq.2}$$

Table 1. Stability in Cell and Ocular Tissue Homogenates-First-Order Degradation Rate Constants of All Prodrugs

Prodrugs	*rPCEC*	*Cornea*	*Aqueous humor*	*ICB*	*Lens*
LV-LV-ACV	11.36 ± 1.32	17.3 ± 1.12	16.3 ± 2.22	14.8 ± 0.7	14.7 ± 1.1
LV-DV-ACV	0.96 ± 0.15	3.9 ± 0.02	3.07 ± 0.03	2.3 ± 0.07	1.22 ± 0.26
DV-LV-ACV	0.75 ± 0.04	2.8 ± 0.05	2.1 ± 0.5	0.7 ± 0.20	0.44 ± 0.002
DV-DV-ACV	ND	ND	ND	ND	ND

Values are represented as $k \times 10^3$ min^{-1} mg^{-1} protein.
Values are mean ± SD ($n = 3$).
ND, no degradation in 24 h; LV-LV-acyclovir, L-valine-L-valine-ACV; LV-DV-ACV, L-valine-D-valine-acyclovir; DV-LV-ACV, D-valine-L-valine-acyclovir; DV-DV-ACV, D-valine-D-valine-acyclovir; rPCEC, rabbit primary corneal epithelial cell; ICB, iris ciliary body.

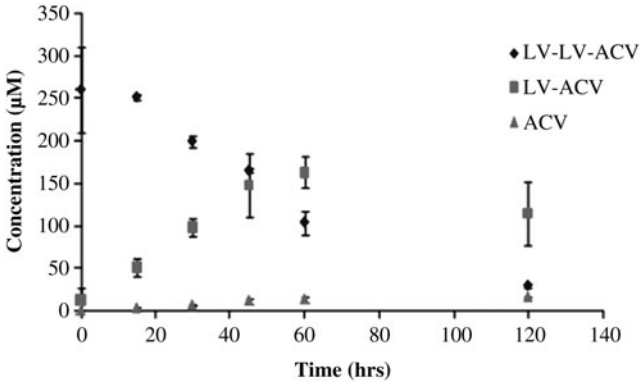

FIG. 1. Bioconversion pathway of LV-LV-ACV in rPCEC homogenate. ACV, acyclovir; LV-LV-ACV, L-valine-L-valine-ACV; rPCEC, rabbit primary corneal epithelial cell.

Particle size analysis by DLS

Dynamic light scattering (Brookhaven Zeta Plus Instrument) technique was applied for the measurement particle size. The polydispersity values were also determined.

Surface morphology analysis by scanning electron microscopy

Surface morphology of nanoparticles with optimum entrapment efficiencies was studied using scanning electron microscopy (FEG ESEM XL 30; FEI). Freeze-dried nanoparticles were attached to a double-sided tape, spray-coated with gold–palladium at 0.6 kV, and finally examined under the electron microscope and photographed.

Table 2. Docking Scores of stereoisomeric Dipeptide Prodrugs of Acyclovir

Name of the prodrug	*Chemical structure*	*Glide score*
LV-LV-ACV	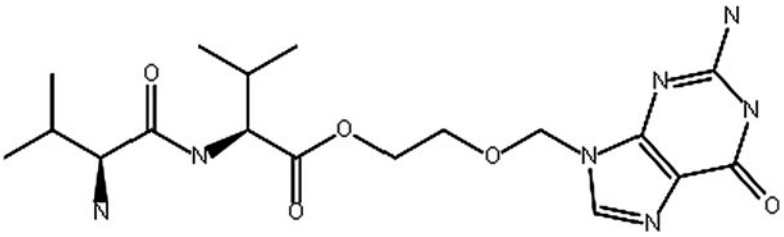	−4.38
LV-DV-ACV	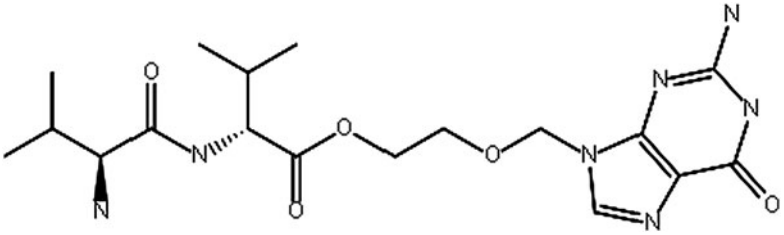	−4.12
DV-LV-ACV	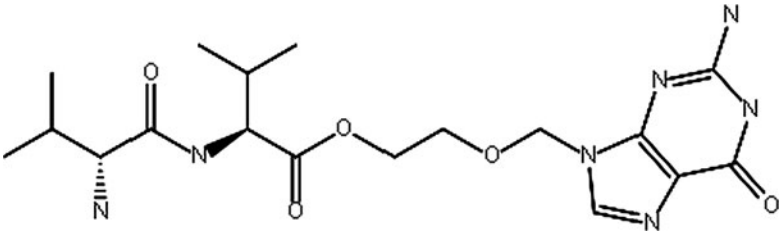	−3.83
DV-DV-ACV	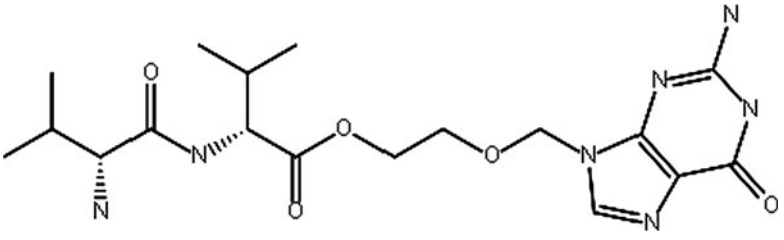	−3.11

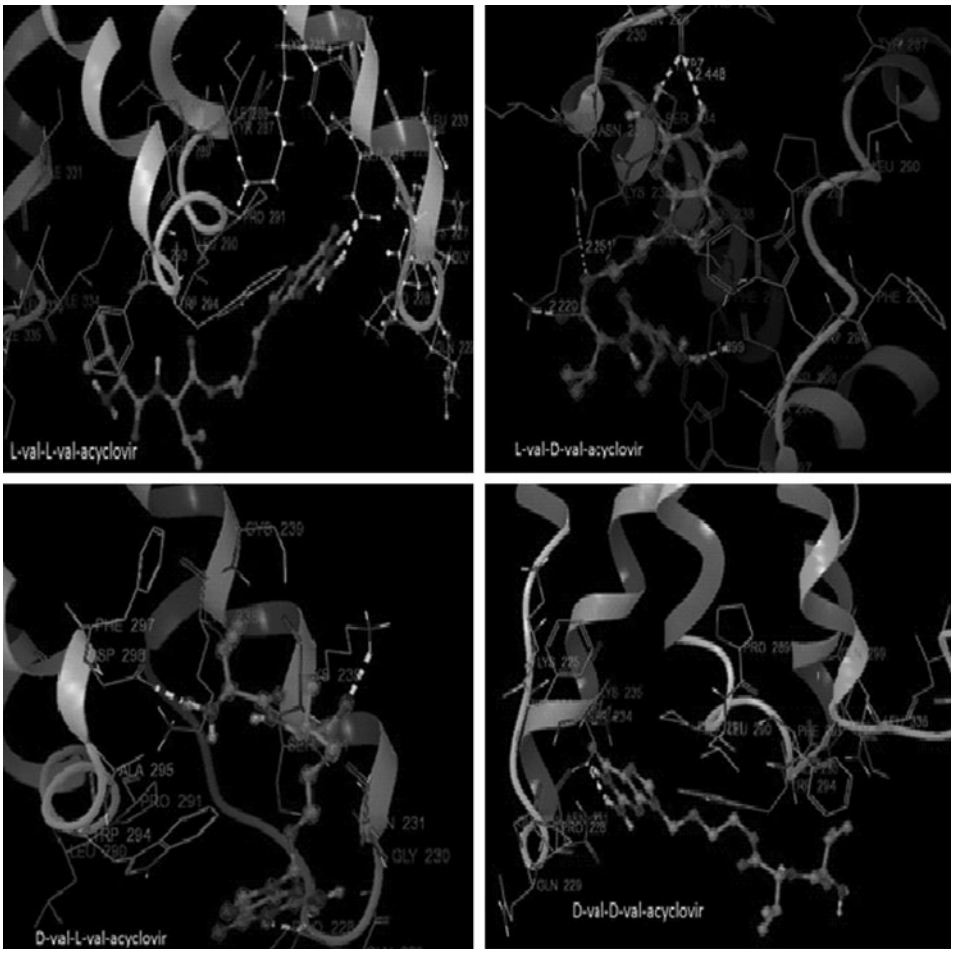

FIG. 2. Binding of stereoisomeric peptide prodrugs of ACV near tryptophan 294 amino acid.

Release of prodrugs from nanoparticles suspended in DPBS and thermosensitive gels

Prodrug loaded nanoparticles (40 mg) were dispersed in 1 mL IPBS, pH 7.4 and, subsequently, introduced into a dialysis bag (MWCO −6275 g/mol). PLGA nanoparticles containing LV-LV-ACV were suspended in 1 mL of 23% w/w PLGA-PEG-PLGA polymer solution and then dialysed. The polymer solution inside the dialysis bag formed gel at 37°C within a period of 30–60 s. The dialysis bags were introduced into vials containing 10 mL IPBS with 0.025% w/v sodium azide added to avoid microbial growth and 0.02% (w/v) Tween 80 to maintain sink condition. The vials were placed in a shaker bath at 37°C ± 0.5°C and 60 oscillations/min. At regular time intervals, 200 μL of samples were withdrawn and

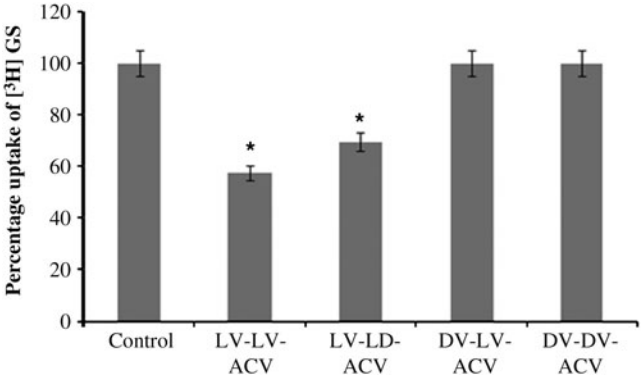

FIG. 3. Percentage uptake of [^{3}H]-Gly-Sar (GS) by rPCEC in presence of LV-LV-ACV, LV-DV-ACV, DV-LV-ACV, and DV-DV-ACV. Values are expressed as percent uptake relative to control ([^{3}H] GS alone). *$P < 0.05$. LV-DV-ACV, L-valine-D-valine-acyclovir; DV-LV-ACV, D-valine-L-valine-acyclovir; DV-DV-ACV, D-valine-D-valine-acyclovir.

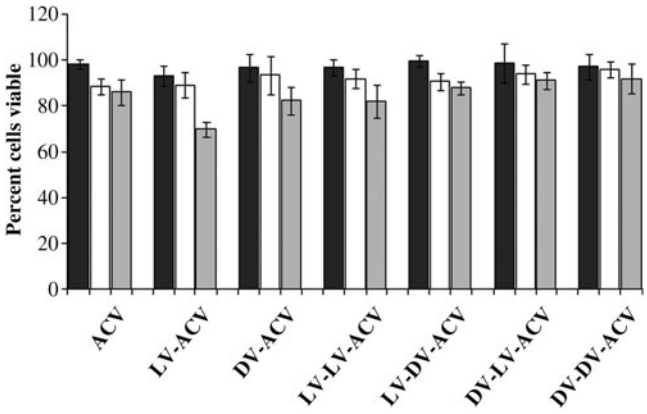

FIG. 4. Cytotoxicity of ACV, LV-ACV, LV-LV-ACV, LV-DV-ACV, DV-LV-ACV, and DV-DV-ACV in rPCECs.

Table 3. Entrapment Efficiency and Drug Content Using Various Grades of PLGA

	LV-LV-ACV		*LV-DV-ACV*	
Various grades of PLGA	*Entrapment efficiency (%)*	*Drug content (%)*	*Entrapment efficiency (%)*	*Drug content (%)*
PLGA50:50	45.7 ± 1.3	4.2 ± 0.2	38.1 ± 1.5	3.9 ± 0.2
PLGA65:35	50.5 ± 2.9	4.7 ± 0.3	54.4 ± 2.3	5.6 ± 0.6
PLGA75:25	59.7 ± 1.4	5.5 ± 0.5	42.7 ± 1.6	4.3 ± 0.3
PLA	52.4 ± 2.0	4.9 ± 0.4	32.7 ± 1.0	3.7 ± 0.1

Studies were conducted from 2 batches ($n = 3$/batch).

replaced with equal volumes of fresh buffer. Release samples were analyzed using HPLC. Similarly, release studies were carried out for PLGA nanoparticles containing LV-DV-ACV alone and when suspended in thermosensitive gels.

Results

The yield, mass, and NMR spectra for LV-LV-ACV, LV-DV-ACV, DV-LV-ACV, and DV-DV-ACV has already been published from our laboratory by Talluri et al.[15] Bioreversion of all the prodrugs (LV-LV-ACV, LV-DV-ACV, DV-LV-ACV, and DV-DV-ACV) was studied in rPCECs and ocular tissue homogenates. Dipeptide prodrugs with D-valine moiety at the terminal position exhibited more stability and were less susceptible to enzymatic degradation. Degradation rate constants of dipeptide prodrugs in rPCEC and rabbit ocular tissue homogenates are shown in Table 1. All prodrugs except DV-DV-ACV exhibited a first-order degradation rate. The descending order of degradation rate constants LV-LV-ACV > LV-DV-ACV > DV-LV-ACV in rPCEC homogenates were found to be $11.36 > 0.96 > 0.75 \text{ k} \times 10^3$ min^{-1} mg^{-1} protein, respectively. The degradation rate constant for the prodrugs in rabbit ocular tissues were found to be in the order of cornea > aqueous humor > iris ciliary body (ICB) > lens. For example, the degradation rate of LV-LV-ACV in cornea > aqueous humor > ICB > lens were found to be $17.3 > 16.32 > 14.8 > 14.7 \text{ k} \times 10^3$ min^{-1} mg^{-1} protein, respectively. A similar trend was observed with LV-DV-ACV and DV-LV-ACV. Peptide prodrugs with 2 D-valine moieties (DV-DV-ACV) were found to be the most stable prodrugs, and no degradation was evident in cell and ocular tissue homogenate studies for 24 h. Bioreversion pathway of LV-LV-ACV in rPCEC homogenates was shown in Fig. 1. LV-LV-ACV bioconversion comprises 2 steps (1) hydrolysis of the peptide bond in the presence of peptidases results in the formation of an amino acid derivative LV-ACV and (2) esterases cleave the ester bond present in LV-ACV to convert into the parent drug ACV. Traces of ACV can be obtained directly from LV-LV-ACV. The docking results indicate that L-valine in the terminal position increases the affinity of the prodrugs to the peptide transporter protein. The binding affinities (glide docking scores) of prodrugs are summarized in Table 2. Binding of stereoisomeric peptide prodrugs of ACV near tryptophan 294 amino acid to peptide transporter are shown in Fig. 2. Uptake of LV-LV-ACV, LV-DV-ACV, DV-LV-ACV, and DV-DV-ACV prodrugs were carried out in rPCECs. All the prodrugs except DV-DV-ACV inhibited the uptake of [^{3}H] GS demonstrating their ability to interact with PEPT (Fig. 3). [^{3}H] GS is a model substrate for peptide transporter. Uptake of [^{3}H] GS (0.5 μCi/mL) was inhibited in the presence of LV-LV-ACV, LV-DV-ACV, and DV-LV-ACV at 1 mM concentration. In this study, it was observed that LV-LV-ACV had significantly inhibited the uptake of [^{3}H] GS across rPCECs demonstrating its affinity toward PEPT. Results obtained from cytotoxicity studies on rPCECs after exposure for 24 h to ACV, LV-ACV, DV-ACV, LV-LV-ACV, LV-DV-ACV, DV-LV-ACV, and DV-DV-ACV are shown in Fig. 4. Blank medium without any drug was selected as the negative control, and 10% v/v DMSO was used as a positive control. Stereoisomeric dipeptide prodrugs did not express any significant cytotoxicity at 1.25, 2.5, and 5 mM concentrations, proving that these compounds are safe and nontoxic. Conjugation of various stereo isomeric dipeptides to ACV did not exhibit any sign of toxicity and were equivalent or even better than parent ACV. Based on the bioreversion, interaction with PEPT transporter, and cytotoxicity results, LV-LV-ACV and LV-DV-ACV were considered to be ideal and used in the preparation of PLGA nanoparticles. Since LV-LV-ACV and LV-DV-ACV are hydrophilic in nature with fairly high water solubility, W/O/W double emulsion solvent evaporation method was used in the preparation of nanoparticles. Entrapment efficiency of LV-LV-ACV and LV-DV-ACV were studied using various grades of PLGA polymers (PLGA 50:50, PLGA 65:35, PLGA 75:25, and PLA). Entrapment efficiencies of LV-LV-ACV with PLGA 50:50, PLGA 65:35, PLGA 75:25, and PLA were found to be 45.7% ± 1.3%, 50.5% ± 2.9%, 59.7% ± 1.4%, and 52.4% ± 2.0%, respectively. Entrapment efficiency and drug loading increased with increasing lactide ratios. However, 100% lactide reduces ratios the entrapment efficiency. Similarly, entrapment efficiencies of LV-DV-ACV with PLGA 50:50, PLGA 65:35, PLGA 75:25, and PLA were found to be 38.1% ± 1.5%, 54.4% ± 2.3%, 42.7% ± 1.6%, and 32.7% ± 1.0%, respectively.

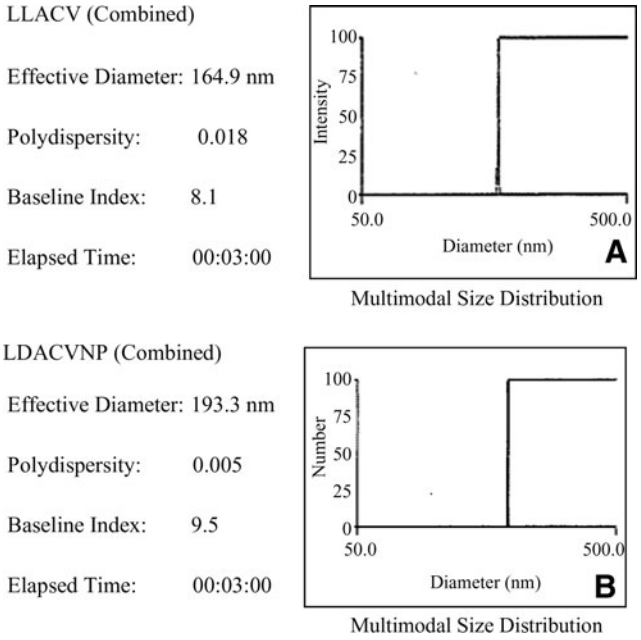

FIG. 5. Particle size distribution curves of nanoparticles. **(A)** PLGA75:25 nanoparticles loaded with LV-LV-ACV and **(B)** PLGA 65:35 nanoparticles loaded with LV-DV-ACV.

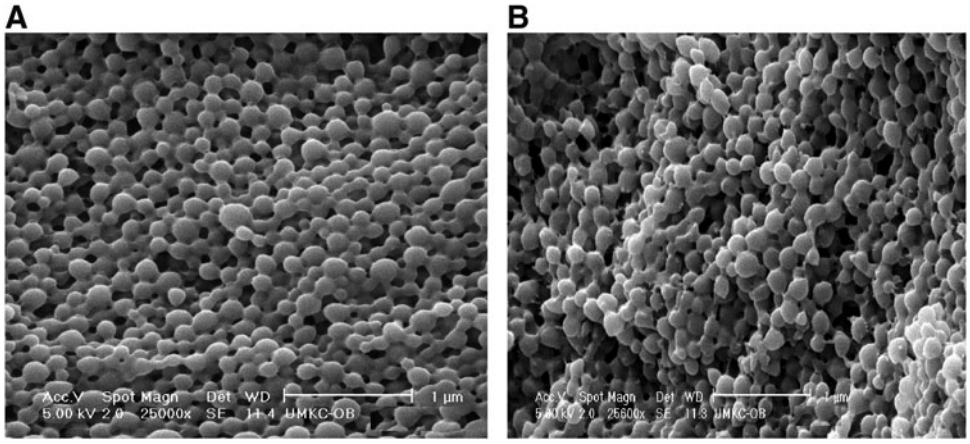

FIG. 6. Surface morphology of nanoparticles. **(A)** PLGA 75:25 nanoparticles loaded with LV-LV-ACV and **(B)** PLGA 65:35 nanoparticles loaded with LV-DV-ACV.

Entrapment efficiency and drug loading of LV-DV-ACV were highest with PLGA 65:35. Table 3 represents all the experimental values of entrapment efficiencies and drug loading. LV-LV-ACV nanoparticles prepared with PLGA 75:25 and LV-DV-ACV nanoparticles prepared with PLGA 65:35 were further characterized for surface morphology, particle size, zeta potential, and *in vitro* release properties. DLS technique and scanning electron microscopy substantiates the size uniformity and spherical shape of the particles with a smooth surface (Figs. 5 and 6). Sizes of LV-LV-ACV and LV-DV-ACV were found to be 164.9 and 193.3 nm, respectively. Nanoparticles exhibited unimodal size distribution with polydispersity values very close to zero. The mean particle size and polydispersity values are shown in Fig. 5. A biphasic release pattern was observed from the LV-LV-ACV and LV-DV-ACV nanoparticles over a duration of 72 h. An initial rapid phase (burst) followed by sustained release was observed in both cases Figs. 7 and 8. Release profiles of LV-LV-ACV and LV-DV-ACV from the formulations prepared by dispersing PLGA 75:25 and PLGA 65:35 nanoparticles in PLGA-PEG-PLGA thermosensitive gel were also obtained. Synthesis and characterization of triblock copolymer PLGA-PEG-PLGA (weight average M_w determined by gel permeation chromatography–4,759 Da) has already been published from our laboratory.[33] Phase-transition studies revealed that polymer concentrations ranging between 20% and 25% w/v form gel at 32°C–60°C.[34] Since the temperature inside the eye ranges from 34.0°C to 37.0°C, such polymeric gels may be appropriate for delivery. Burst release of active ingredients has been considerably retarded when nanoparticles were dispersed in thermosensitive gels. Moreover, a clear zero-order release pattern was observed for the drug from these formulations (Figs. 7 and 8). Burst release of LV-LV-ACV and LV-DV-ACV has been considerably retarded when nanoparticles are dispersed in thermosensitive gels. Dispersion of polymeric nanoparticles in PLGA-PEG-PLGA sustained the release of the prodrug over a period of 1 week.

Discussion

It is a well-known fact that on topical administration, ACV formulations may not achieve optimal therapeutic concentrations in the target sites due to low water solubility and membrane permeability.[35] Novel stereoisomeric dipeptide prodrugs of ACV were developed, and the effect of stereoisomerism on enzymatic stability was studied in various rabbit ocular tissues and rPCEC homogenates. Results from the hydrolysis study indicated that incorporation of 2 D-isomers can significantly improve the stability of prodrugs.[15] However, D-isomers can

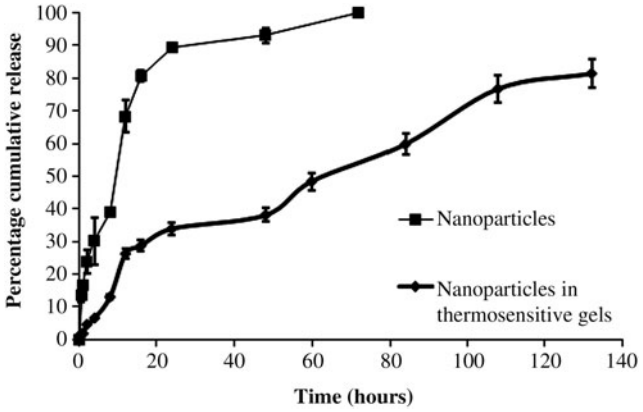

FIG. 7. *In vitro* release profile of LV-LV-ACV from PLGA75:25 nanoparticles and LV-LV-ACV from PLGA75:25 nanoparticles suspended in PLGA-PEG-PLGA thermosensitive gel. Each data point is the average of 3 samples. Error bars represent the standard error of mean.

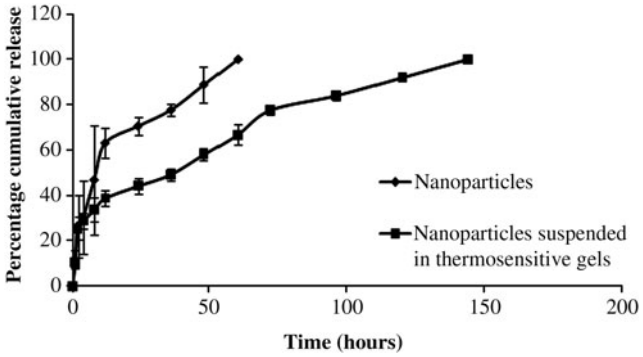

FIG. 8. *In vitro* release profile of LV-DV-ACV from PLGA65:35 nanoparticles and DVACV from PLGA65:35 nanoparticles suspended in PLGA-PEG-PLGA thermosensitive gel. Each data point represents an average of 3 samples. Error bars represent the standard error of mean.

also lower affinity toward PEPT. The increase in the stability on incorporation of D-valine may be attributed to reduced affinity toward hydrolytic enzymes. Previous reports from Anand et al.[10] clearly explained the bioconversion mechanism of dipeptide prodrugs. The dipeptide bond is hydrolyzed by the peptidases resulting in the regeneration of amino acid ester of ACV, which is further hydrolyzed by esterases regenerating the parent ACV. The regeneration of ACV directly from dipeptide prodrug may occur to a smaller extent. *In vitro* uptake studies of LV-LV-ACV, LV-DV-ACV, DV-LV-ACV, and DV-DV-ACV were carried out in rPCECs.[9] LV-LV-ACV and LV-DV-ACV had shown high PEPT affinity, whereas DV-LV-ACV and DV-DV-ACV did not show any affinity. This result indicates that D-valine moiety in the terminal position is not recognized by peptide transporter. Hence, both DV-LV-ACV and DV-DV-ACV did not show any affinity toward peptide transporter on rPCEC line. Cell cytotoxicity studies suggest that all the prodrugs are safe and nontoxic.[9] Ideal prodrugs should enter the cornea via peptide transporter and readily convert to parent drug in the tissue before elimination through aqueous humor. Bioconversion half life of prodrugs should be less than the *in vivo* elimination of half life. Previous studies from our laboratory by Anand et al.[36] concluded that the half life of cumulative ACV from the dipeptide prodrugs was calculated as $\sim$180 min. Based on these data, we have concluded that LV-LV-ACV and LV-DV-ACV are suitable peptide ACV prodrugs for further formulation studies. Owing to the appreciable PEPT1 affinity, we anticipate that LV-LV-ACV and LV-DV-ACV could be readily absorbed across the corneal epithelium and then get converted to ACV for the treatment of severe HSV infections in deeper corneal tissues such as stroma.

LV-LV-ACV and LV-DV-ACV were loaded into PLGA nanoparticles, which, in turn, were dispersed in thermosensitive gels to overcome the disadvantages associated with conventional eye drops. Dipeptide prodrug-loaded nanoparticles dispersed in thermosensitive gels may prevent precorneal degradation of prodrugs and overcome the precorneal drainage associated with rapid blinking, lachrymation, and drainage. A series of PLGA polymers of varying lactide/glycolide ratios were employed in the preparation of nanoparticles. Entrapment efficiency values of LV-LV-ACV and LV-DV-ACV were observed to be significantly higher with PLGA 75:25 and PLGA 65:35 polymers, respectively. This result can be attributed to stronger interactions of LV-LV-ACV and LV-DV-ACV with PLGA 75:25 and PLGA 65:35 polymers, respectively. Nanoparticles containing LV-LV-ACV and LV-DV-ACV exhibited uniform size distribution with low polydispersity. *In vitro* prodrug release from nanoparticles exhibited a biphasic pattern with an initial burst phase followed by a sustained release phase. Dispersion of nanoparticles in thermosensitive gels completely eliminated the burst release. This may be due to the adhesion of thermo gelling polymer to nanoparticle surface.[12] Such nanoparticulate formulations may provide sustained release of LV-LV-ACV and LV-DV-ACV after topical administration. Moreover, this formulation remains in solution form at room temperature and forms a gel at eye temperature after topical administration. Moreover, gel also prevents the rapid drainage of nanoparticles, interaction of prodrugs with tear proteins, tear dilution of prodrugs, and prodrug metabolism after topical delivery to the eye.[37] On topical administration, nanoparticles suspended in thermosensitive gels form a depot in the cul-de-sac providing a robust concentration gradient for efficient permeation of prodrugs across the cornea in a sustained manner.

For patients suffering from superficial keratitis, LV-LV-ACV loaded nanoparticles may be more appropriate. Superficial keratitis affects the superficial corneal layers. LV-LV-ACV released from the formulation penetrates the superficial corneal layers and regenerates quickly to ACV for action against HSV-1 infection. Stromal keratitis mainly affects the deeper layers of the cornea. LV-DV-ACV loaded nanoparticles may be more effective in the treatment of stromal keratitis. LV-DV-ACV will be metabolically stable enough to penetrate deeper layers of cornea and regenerate the active or parent drug in the deeper layers of the cornea. Hence, prodrug-entrapped nanoparticles formulations can be selectively applied depending on the severity of infection. Moreover, a cocktail of LV-LV-ACV and LV-DV-ACV nanoparticles can also be indicated in patients with deeper and wide spread HSV-1 ocular infections.

Conclusion

LV-LV-ACV and LV-DV-ACV appear to be very suitable ACV peptide prodrugs in terms of stability, bioreversion, cytotoxicity, and affinity toward rabbit PEPT1 transporter. After translocation across the cornea via PEPT transporter, prodrugs are expected to revert rapidly into their parent drug. Entrapment of LV-LV-ACV and LV-DV-ACV in PLGA nanoparticles may retard the degradation of prodrugs in the precorneal area and further sustain the release in deep corneal tissues. Dispersion of nanoparticles in the PLGA-PEG-PLGA thermosensitive gel may significantly eliminate the burst release of prodrugs and overcome the problems such as drug loss by tear turnover, tears dilution, and blink reflex, thus causing rapid extensive loss on topical administration into the cul-de-sac. *In vivo* pharmacokinetic studies need to be carried out to determine the aqueous humor kinetics of these formulations after topical administration.

Acknowledgments

The authors are thankful to Dr. Vladimir Dusevich, School of Dentistry, for assisting with the operation of scanning electron microscopic studies; Dr. Elisabet Kostoryz, School of Dentistry, for helping us in using dynamic light scattering studies. This work was supported by Missouri Life Sciences Grant, and NIH grants R01 EY 09171-16 and R01 EY 10659-14.

Author Disclosure Statement

No competing financial interests exist.

References

1. Toma, H.S., et al. Ocular HSV-1 latency, reactivation and recurrent disease. *Semin. Ophthalmol.* 23:249–273, 2008.
2. Shimomura, Y. [Herpes simplex virus latency, reactivation, and a new antiviral therapy for herpetic keratitis]. *Nippon Ganka Gakkai Zasshi* 112:247–264; discussion 265, 2008.
3. Liesegang, T.J. Ocular herpes simplex infection: pathogenesis and current therapy. *Mayo Clin. Proc.* 63:1092–1105, 1988.
4. Wander, A.H. Herpes simplex and recurrent corneal disease. *Int. Ophthalmol. Clin.* 24:27–38, 1984.

5. Turner, J., et al. Influence of increased age on the development of herpes stromal keratitis. *Exp. Gerontol.* 38:1205–1212, 2003.
6. Jabs, D.A. Acyclovir for recurrent herpes simplex virus ocular disease. *N. Engl. J. Med*. 339:340–341, 1998.
7. Falcon, M.G. Herpes simplex virus infections of the eye and their management with acyclovir. *J. Antimicrob. Chemother*. 12 Suppl B:39–43, 1983.
8. Hughes, P.M., and Mitra, A.K. Effect of acylation on the ocular disposition of acyclovir. II: corneal permeability and anti-HSV 1 activity of 2′-esters in rabbit epithelial keratitis. *J. Ocul. Pharmacol.* 9:299–309, 1993.
9. Anand, B.S., and Mitra, A.K. Mechanism of corneal permeation of L-valyl ester of acyclovir: targeting the oligopeptide transporter on the rabbit cornea. *Pharm. Res.* 19:1194–1202, 2002.
10. Anand, B., Nashed, Y., and Mitra, A. Novel dipeptide prodrugs of acyclovir for ocular herpes infections: bioreversion, antiviral activity and transport across rabbit cornea. *Curr. Eye. Res.* 26:151–163, 2003.
11. Gulsen, D., and Chauhan, A. Ophthalmic drug delivery through contact lenses. *Invest. Ophthalmol. Vis. Sci.* 45:2342–2347, 2004.
12. Boddu, S.H., et al. Novel nanoparticulate gel formulations of steroids for the treatment of macular edema. *J. Ocul. Pharmacol. Ther.* 26:37–48, 2010.
13. de Campos, A.M., et al. Chitosan nanoparticles as new ocular drug delivery systems: in vitro stability, in vivo fate, and cellular toxicity. *Pharm. Res.* 21:803–810, 2004.
14. Nashed, Y.E., and Mitra, A.K. Synthesis and characterization of novel dipeptide ester prodrugs of acyclovir. *Spectrochim. Acta. A Mol. Biomol. Spectrosc.* 59:2033–2039, 2003.
15. Talluri, R.S., et al. Synthesis, metabolism and cellular permeability of enzymatically stable dipeptide prodrugs of acyclovir. *Int. J. Pharm.* 361:118–124, 2008.
16. Agarwal, S., et al. Peptide prodrugs: improved oral absorption of lopinavir, a HIV protease inhibitor. *Int. J. Pharm.* 359:7–14, 2008.
17. Katragadda, S., et al. Ocular pharmacokinetics of acyclovir amino acid ester prodrugs in the anterior chamber: evaluation of their utility in treating ocular HSV infections. *Int. J. Pharm.* 359:15–24, 2008.
18. Tak, R.V., et al. Transport of acyclovir ester prodrugs through rabbit cornea and SIRC-rabbit corneal epithelial cell line. *J. Pharm. Sci.* 90:1505–1515, 2001.
19. www.uniprot.org/uniprot/P36836.
20. Zhang, Y. I-TASSER: fully automated protein structure prediction in CASP8. *Proteins* 77 Suppl 9:100–113, 2009.
21. Roy, A., Kucukural A., and Zhang, Y. I-TASSER: a unified platform for automated protein structure and function prediction. *Nat. Protoc.* 5:725–738, 2010.
22. Zhang, Y. I-TASSER server for protein 3D structure prediction. *BMC Bioinform.* 9:40, 2008.
23. Prime, v. 2.1, and L. Schrödinger. New York, 2010.
24. Jorgensen, W., and Tirado-Rives, J. The OPLS force field for proteins. Energy minimizations for crystals of cyclic peptides and crambin. *J. Am. Chem. Soc.* 110:1657–1666, 1988.
25. Maestro, *version 9.0*. New York: L. Schrödinger; 2010.
26. Ligprep, *version 2.3*. New York: L. Schrödinger; 2010.
27. Glide, *version 5.5.* New York: L. Schrödinger; 2010.
28. Meredith, D., and Price, R.A. Molecular modeling of PepT1—towards a structure. *J. Membr. Biol*. 213:79–88, 2006.
29. Glide 5.5. *User Manual*. New York: L. Schrödinger; 2010.
30. Friesner, R.A., et al. Glide: a new approach for rapid, accurate docking and scoring. 1. Method and assessment of docking accuracy. *J. Med. Chem.* 47:1739–1749, 2004.
31. Katragadda, S., Talluri, R.S., and Mitra, A.K. Modulation of P-glycoprotein-mediated efflux by prodrug derivatization: an approach involving peptide transporter-mediated influx across rabbit cornea. *J. Ocul. Pharmacol. Ther.* 22:110–120, 2006.
32. Vandervoort, J., and Ludwig, A. Biocompatible stabilizers in the preparation of PLGA nanoparticles: a factorial design study. *Int. J. Pharm*. 238:77–92, 2002.
33. Wagstaff, A.J., Faulds, D., and Goa, K.L. Aciclovir. A reappraisal of its antiviral activity, pharmacokinetic properties and therapeutic efficacy. *Drugs* 47:153–205, 1994.
34. Duvvuri, S., Janoria, K.G., and Mitra, A.K. Development of a novel formulation containing poly(d,l-lactide-co-glycolide) microspheres dispersed in PLGA-PEG-PLGA gel for sustained delivery of ganciclovir. *J. Control Release* 108:282–293, 2005.
35. Cortesi, R., and Esposito, E. Acyclovir delivery systems. *Expert Opin. Drug Deliv*. 5:1217–1230, 2008.
36. Anand, B.S., et al. In vivo ocular pharmacokinetics of acyclovir dipeptide ester prodrugs by microdialysis in rabbits. *Mol. Pharm.* 3:431–440, 2006.
37. Kaur, I.P., and Kanwar, M. Ocular preparations: the formulation approach. *Drug Dev. Ind. Pharm*. 28:473–493, 2002.

Received: December 17, 2010
Accepted: February 23, 2011

Address correspondence to:
Dr. Ashim K. Mitra
Division of Pharmaceutical Sciences
School of Pharmacy
University of Missouri-Kansas City
2464 Charlotte St.
Kansas City, MO 64108-2718

E-mail: mitraa@umkc.edu